ISSN 0965-5425, Computational Mathematics and Mathematical Physics, 2017, Vol. 57, No. 10, pp. 1720–1733. © Pleiades Publishing, Ltd., 2017.
Original Russian Text © V.R. Efremov, A.S. Kozelkov, A.V. Kornev, A.A. Kurkin, V.V. Kurulin, D.Yu. Strelets, N.V. Tarasova, 2017, published in Zhurnal Vychislitel'noi Matematiki i Matematicheskoi Fiziki, 2017, Vol. 57, No. 10, pp. 1748–1762.

Method for Taking into Account Gravity in Free-Surface Flow Simulation

V. R. Efremov[a,*], A. S. Kozelkov[b,], A. V. Kornev[c,***], A. A. Kurkin[b,****], V. V. Kurulin[d,*****], D. Yu. Strelets[c,******], and N. V. Tarasova[d,*******]**

[a] *Shipunov Instrument Design Bureau, Tula, 300001 Russia*

[b] *Nizhny Novgorod State Technical University, Nizhny Novgorod, 603950 Russia*

[c] *Moscow State Aviation Institute, Moscow, 125993 Russia*

[d] *Russian Federal Nuclear Center All-Russia Research Institute of Experimental Physics, Sarov, Nizhny Novgorod oblast, 607188 Russia*

** e-mail: valentin_e@mail.r*

*** e-mail: askozelkov@mail.r*

**** e-mail: avkornev@mai.ru*

***** e-mail: aakurkin@gmail.com*

****** e-mail: kurulin@mail.r*

******* e-mail: dimstrelets@rambler.ru*

******** e-mail: tara@vniief.ru*

Received February 13, 2017

Abstract—A numerical algorithm that correctly takes into account the force of gravity in the presence of density discontinuities is constructed using unstructured collocated grids and splitting algorithms based on SIMPLE-type methods. A correct hydrostatic pressure field is obtained by explicitly extracting the gravity force contribution to the pressure equation and computing it using the solution of the gravity equilibrium problem for a two-phase medium. To ensure that the force of gravity is balanced by the pressure gradient in the case of a medium at rest, an algorithm is proposed according to which the pressure gradient in the equations of motion is replaced by a modification allowing for the force of gravity. Well-known free-surface problems are used to show that, in contrast to previously known algorithms, the proposed ones on unstructured meshes correctly predict hydrostatic pressure fields and do not yield velocity oscillations or free-surface distortions.

Keywords: free surface, gravity, VOF method, finite-volume method, numerical scheme

DOI: 10.1134/S0965542517100086

INTRODUCTION

At present, free-surface multiphase flows can be simulated by applying several methods that differ in the approach to free-surface computation. One method is based on the Lagrangian approach, in which a free surface is tracked using grid nodes or particles (see [1, 2]). Another method is based on the Euler approach, in which a free surface is tracked using special markers, which can be particles (see [3]) or spatial marker functions governed by the convective transport equation [4–6]. Most frequently used in practice is the latter method with the marker function being the volume fraction of the fluid (volume-of-fluid (VOF) method [6]). In this method, the fluid–gas system is treated as a unified one-speed medium with variable physical properties. The method can easily be extended to arbitrary unstructured meshes and an arbitrary number of phases [7].

A crucial characteristic for free-surface flows is gravity. It has a discontinuity at the free surface due to a sharp change in the material density. As a result, the pressure gradient, which balances gravity in the case of a medium at rest, suffers a discontinuity as well [8]. The design of a numerical algorithm for taking into account gravity and computing the pressure gradient is a nontrivial problem. This is especially true in the case of collocated grids, which are mainly used in practice, but lead to a weak coupling between the velocity and pressure fields [9–11]. In collocated grids, pressure and velocity are stored at the same locations

(as a rule, at cell centers). This leads to checkerboard oscillations, which can be avoided by applying, for example, the Rhie–Chow method [12].

The construction of numerical algorithms free of spurious oscillations in the case of an inhomogeneous gravity field caused by density inhomogeneities has been addressed in numerous publications (see, e.g., [13–15]). Specifically, allowance for a body force (an example of which is gravity) in the momentum conservation equation was discussed in [13]. To eliminate oscillations from the velocity and pressure fields, the authors proposed a correction term of the Rhie–Chow type, [2] which solves the problem. However, they did not consider strong discontinuities in the body force field, in which case the pressure gradient has to be calculated so as to completely balance the body force when the medium is at rest.

Allowance for gravity was theoretically considered in [14]. Relying on the ideas of [13], a balance-ensuring expression was proposed for interpolating the body force and pressure to internal grid faces. The velocity field was demonstrated to have no oscillations, but the resulting shapes of the free surface were not discussed. Additionally, the efficiency of the algorithm in the case of arbitrary unstructured meshes was not analyzed. Note also that the Rhie–Chow correction term proposed in [16] was used in [14] for the nonstationary term in the momentum conservation equation. However, it was shown in [17] that this correction may lead to a distorted free surface shape.

To calculate the pressure gradient in the presence of gravity forces, an efficient scheme based on the interpolation of the pressure gradient with allowance for the medium densities in adjacent cells was presented in [15]. This algorithm was free of spurious oscillations in the velocity field near the free surface, but its performance was demonstrated only on orthogonal grids with lines parallel to the direction of the gravity force.

In this paper, we describe an algorithm for deriving a pressure equation based on the Rhie–Chow method. The algorithm is constructed by replacing the interpolation of the gravity force in the pressure equation by its direct discrete analogue. An expression for the direct discrete analogue is obtained using the hydrostatic approximation, which ensures that a correct pressure field is produced on an arbitrary unstructured mesh. To ensure the balance between the gravity force and the pressure gradient in the case of a medium at rest, an algorithm is proposed based on replacing the pressure gradient in the equation of motion by its modification taking into account the force of gravity.

The efficiency of the proposed solutions is examined by numerically solving an equilibrium problem for a two-phase medium under gravity that has an analytical solution. It is shown that, in contrast to existing numerical schemes, the proposed ones yield a correct hydrostatic pressure and ensure the balance between the gravity force and the pressure gradient on unstructured grids. The accuracy of the free surface shape predicted by applying the proposed numerical algorithms is estimated by solving the problem of fluid oscillation under gravity and the breaking liquid column problem.

1. METHOD FOR TAKING INTO ACCOUNT GRAVITY

In the VOF method, the continuity and momentum equations are the same for all phases and are solved for a resulting medium whose properties depend linearly on the volume fraction of each phase. The general system of equations for the multiphase medium has the form (see [7])

$$\begin{cases} \rho\dfrac{\partial u_i}{\partial t}+\dfrac{\partial \rho u_i u_j}{\partial x_j}-u_i\dfrac{\partial \rho u_j}{\partial x_j}=-\dfrac{\partial p}{\partial x_i}+\dfrac{\partial}{\partial x_j}\left(\mu\left(\dfrac{\partial u_i}{\partial x_j}+\dfrac{\partial u_j}{\partial x_i}\right)\right)+\rho g_i, \\ \dfrac{\partial u_i}{\partial x_i}=0, \\ \dfrac{\partial F_j}{\partial t}+u_i\dfrac{\partial F_j}{\partial x_i}=0, \quad j=1\ldots N-1, \quad F_N=1-\sum\limits_{j}^{N-1}F_j, \end{cases} \tag{1.1}$$

where $\rho=\sum_j^N F_j\rho_j$ is the resulting density of the medium, $\mu=\sum_j^N F_j\mu_j$ is the resulting viscosity of the medium, p is the pressure, u_i is the vector of velocity components, N is the number of phases in the problem, F_j is the volume fraction of phase j, and g_i is the force of gravity. In system (1.1), the momentum equation is written so as to produce the best results in the numerical solution of free-surface problems [18].

System (1.1) is solved using classical splitting algorithms, such as SIMPLE [9, 11], PISO [7, 17], and a fully implicit algorithm [19–22]; in all of them, a pressure equation is derived by substituting a discretized velocity equation into the continuity equation. In the case of finite-volume discretization, the discrete

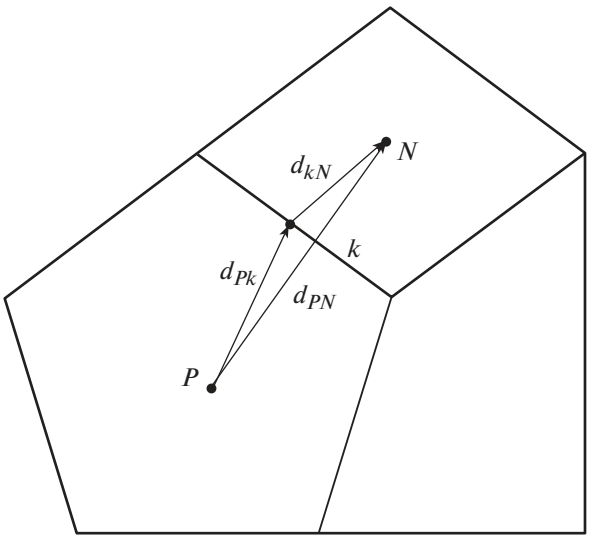

Fig. 1. Two adjacent grid cells.

analogue of the velocity equation is reduced to a system of linear algebraic equations (SLAE) of the form (see [11])

$$a_{PP}u_{i,P} + \sum_k a_{PN}u_{i,N} = R_{i,P} - \left(\frac{\partial p}{\partial x_i}\right)_P V_P, \tag{1.2}$$

where a_{PP} is the diagonal coefficient of the equation for the cell P, a_{PN} is the coefficient miltiplying the velocity in the adjacent cell N separated by the face k, the sum extends over all internal faces, and V_P is the volume of the cell P (Fig. 1).

The right-hand side $R_{i,P}$ includes the explicit part of the discretized convective, diffusion, and nonstationary terms. From Eq. (1.2), the velocity is expressed as

$$u_{i,P} = \frac{1}{a_{PP}}\left(R_{i,P} - \sum_k a_{PN}u_{i,N}\right) - \frac{V_P}{a_{PP}}\left(\frac{\partial p}{\partial x_i}\right)_P = H_{i,P} - \frac{V_P}{a_{PP}}\left(\frac{\partial p}{\partial x_i}\right)_P. \tag{1.3}$$

The velocity $u_{i,k}$ on face k is calculated by interpolating expression (1.3) from the cell centers to the center of face k with weight λ_k, except for the pressure gradient, whose contribution is replaced by its direct discrete analogue [7, 14]. The resulting velocity expression is substituted into the discrete continuity equation (1.1):

$$\sum_k u_{i,k}n_iS_k = \sum_k\left[\left[\lambda_k H_{i,P} + (1-\lambda_k)H_{i,N}\right]n_iS_k - \left(\lambda_k\frac{V_P}{a_{PP}} + (1-\lambda_k)\frac{V_N}{a_{NN}}\right)\frac{p_N - p_P}{d_{PN}}S_k\right] = 0, \tag{1.4}$$

where $u_{i,k}$ is the velocity on face k, n_i is the normal to face k, S_k is the area of face k, and the sum extends over all faces of the cell P. In practice, the weight λ_k is determined in various manners, for example, using the geometric distance from the cell center to the face center [10], applying the diagonal coefficients a_{PP} and a_{PN} [12], or setting $\lambda_k = 0.5$.

Equation (1.4) is used to determine the pressure field at the center of each cell. When the system is in equilibrium, the pressure field must have a hydrostatic distribution (see [8]). However, the pressure distribution determined by Eq. (1.4) depends on the method for interpolating the vector H_i to cell faces, which implicitly involves the contribution of the gravity force ρg_i; as a result, the hydrostatic pressure field can be reproduced incorrectly (see [14]).

In this paper, an algorithm for obtaining a correct hydrostatic pressure at cell centers in the case of a discontinuous density field is designed by extracting the gravity force contribution (along with the pressure gradient) from the right-hand side $R_{i,P}$. With the force of gravity extracted explicitly, Eqs. (1.2)–(1.4) become

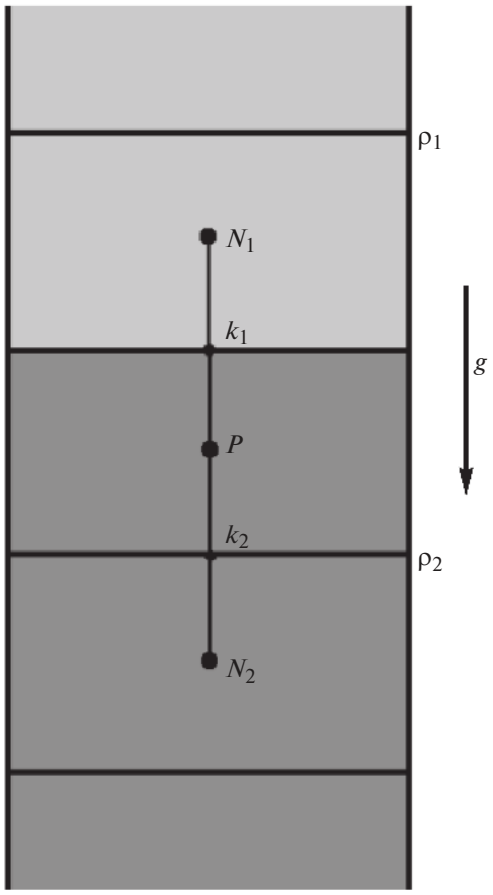

Fig. 2. Equilibrium of the system under gravity.

$$u_{i,P} = H_{i,P} - \frac{V_P}{a_{PP}}\left(\frac{\partial p}{\partial x_i}\right)_P + \frac{V_P}{a_{PP}}\rho g_i, \tag{1.5}$$

$$\sum_k u_{i,k} n_i S_k = \sum_k \left[H_{i,k} n_i S_k - A_k \frac{p_N - p_P}{d_{PN}} S_k + A_k (\rho g_i)_k n_i S_k \right] = 0, \tag{1.6}$$

where $H_{i,\,k} = \lambda_k H_{i,\,P} + (1-\lambda_k) H_{i,\,N}$ and $A_k = \lambda_k \dfrac{V_P}{a_{PP}} + (1-\lambda_k)\dfrac{V_N}{a_{NN}}$.

In this case, pressure equation (1.6) involves the force of gravity interpolated to face k, namely, $(\rho g_i)_k$. To determine its value (which makes it possible to obtain a correct pressure distribution), we consider a one-dimensional model problem of a system at rest consisting of two fluids under gravity with different densities (Fig. 2).

In equilibrium, the velocities in the system are zero, so pressure equation (1.6) becomes

$$A_{k_1}\left(\frac{p_{N_1} - p_P}{d_{PN_1}} - (\rho g)_{k_1}\right) S_{k_1} - A_{k_2}\left(\frac{p_{N_2} - p_P}{d_{PN_2}} - (\rho g)_{k_2}\right) S_{k_2} = 0. \tag{1.7}$$

Equation (1.7) shows that the term $(\rho g)_{k_1}$ directly determines the pressure drop between the centers of the cells P and N_1, while the term $(\rho g)_{k_2}$, between the centers of the cells P and N_2. These pressure drops are calculated analytically (see [8]) assuming that the density inside the cells is constant; as a result,

$$p_{N_1} - p_P = g(d_{N_1 k_1}\rho_1 + d_{k_1 P}\rho_2), \tag{1.8}$$

where $d_{N_1k_1}$ is the distance from the center of the cell N_1 to face k_1 and d_{k_1P} is the distance from face k_1 to the center of the cell P. In view of this, Eq. (1.7) becomes

$$A_{k_1}\left(\frac{p_{N_1}-p_P}{d_{PN_1}}-g\frac{d_{N_1k_1}\rho_1+d_{k_1P}\rho_2}{d_{PN_1}}\right)S_{k_1}-A_{k_2}\left(\frac{p_{N_2}-p_P}{d_{PN_2}}-g\frac{d_{N_2k_2}\rho_1+d_{k_2P}\rho_2}{d_{PN_2}}\right)S_{k_2}=0. \tag{1.9}$$

Obviously, the solution of Eq. (1.9) leads to a pressure drop corresponding to the hydrostatic solution of problem (1.8).

In the three-dimensional case, the hydrostatic pressure drop between the adjacent cells P and N is given by the expression

$$p_N-p_P=d_{i,Nk}g_i\rho_N+d_{i,kP}g_i\rho_P. \tag{1.10}$$

In view of (1.10), Eq. (1.6) can be written as

$$\sum_k u_{i,k}n_iS_k=\sum_k\left[H_{i,k}n_iS_k-A_k\frac{p_N-p_p}{d_{PN}}S_k+A_kd_{i,Nk}g_i\rho_N\right]=0. \tag{1.11}$$

Equation (1.11) ensures the computation of a correct hydrostatic pressure field at cell centers in the case of any method for interpolating the vector H_i to faces.

2. ALGORITHM FOR COMPUTING THE PRESSURE GRADIENT

To ensure that the gravity force is balanced by the pressure gradient in the case of a free surface at rest, the pressure gradient also has to be correctly computed near the free surface. It was shown in [14] that the pressure gradient produced by usual methods (e.g., the Gauss formula [10] or the least squares method) leads to incorrect results, since the pressure field has a kink on the free surface. This difficulty was eliminated in [15] by using the Gauss formula with a modified expression for pressure interpolation to internal faces of P:

$$\left(\frac{\partial p}{\partial x_i}\right)_P=\frac{1}{V_P}\sum_k p_kS_{i,k}, \tag{2.1}$$

$$p_k=\xi\left(\frac{p_Pd_{kN}\rho_N+p_Nd_{Pk}\rho_P}{d_{kN}\rho_N+d_{Pk}\rho_P}\right)+(1-\xi)\left(\frac{p_Pd_{kN}+p_Nd_{Pk}}{d_{kN}+d_{Pk}}\right), \tag{2.2}$$

where $\xi=\cos^2\alpha$ and α is the angle between the normal to face k and the direction of the gravity force. By following this approach, the pressure gradient can be correctly estimated near the free surface in the case of an orthogonal grid with lines parallel to the direction of the gravity force. However, it will be shown below that expression (2.2) yields an unsatisfactory result in the case of an unstructured mesh.

In this work, we use another method, which produces good results on grids of any type. The basic idea behind the method is that the pressure gradient does not need to be calculated directly to solve the equation of motion; instead, it is sufficient to calculate the joint contribution made by the pressure gradient and the force of gravity. To derive such an expression, we introduce a variable p^* representing a modified pressure field:

$$\frac{\partial p^*}{\partial x_i}=\frac{\partial p}{\partial x_i}-\rho g_i. \tag{2.3}$$

To compute the right-hand side of Eq. (1.5) with the newly introduced variable, we consider the integral of (2.3) over the volume of the cell P:

$$\int_{V_P}\frac{\partial p^*}{\partial x_i}dV=\int_{V_P}\frac{\partial p}{\partial x_i}dV-\int_{V_P}\rho g_idV.$$

Passing to a surface integral gives

$$\int_{V_P}\frac{\partial p^*}{\partial x_i}dV=\int_{S_P}(p-G)n_idS, \tag{2.4}$$

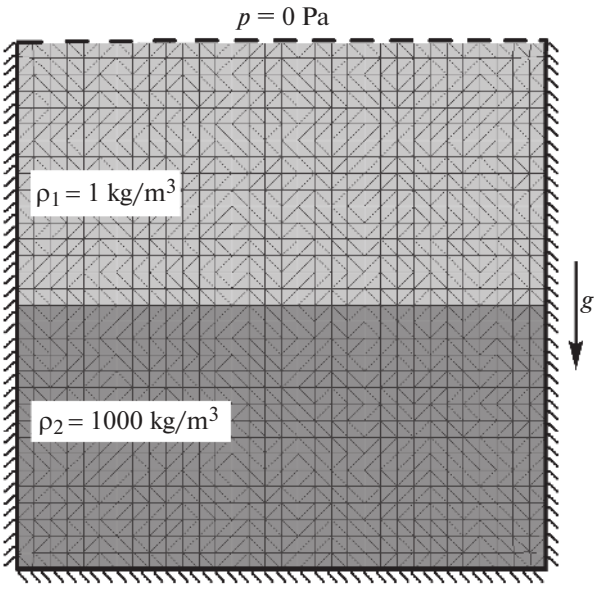

Fig. 3. Conditions of the problem, geometry, and grid.

where G is a primitive of the function ρg_i. Assuming that the density inside the cells is a constant, G can be written as

$$G = \rho g_i r_i + C, \tag{2.5}$$

where r_i is the position vector and C is an arbitrary constant. Due to the presence of C, we can choose an arbitrary starting point for the vector r_i. For the cell P, it is placed at the cell center. Then

$$G = \rho g_i (r_i - r_{P,i}). \tag{2.6}$$

Substituting (2.5) into (2.4) and applying the finite-volume discretization (2.6) yields

$$\int_{V_P} \frac{\partial p^*}{\partial x_i} dV = \int_{S_P} (p - \rho g_i (r_i - r_{P,i})) n_i dS \approx \sum_k [p - \rho g_i (r_i - r_{P,i})]_k n_{k,i} S_k.$$

The second term in square brackets in the last expression is the contribution made to the total pressure by the hydrostatic pressure calculated with respect to the center of cell P. It vanishes at the center of P, while, at the center of the neighboring cell N, it is calculated according to expression (1.10), which is used

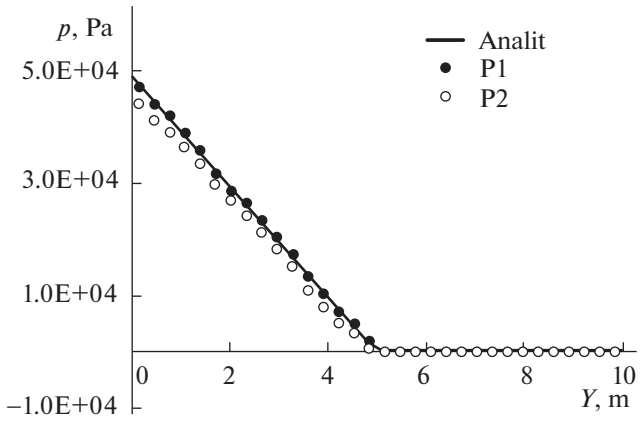

Fig. 4. Pressure produced by the schemes P1 and P2.

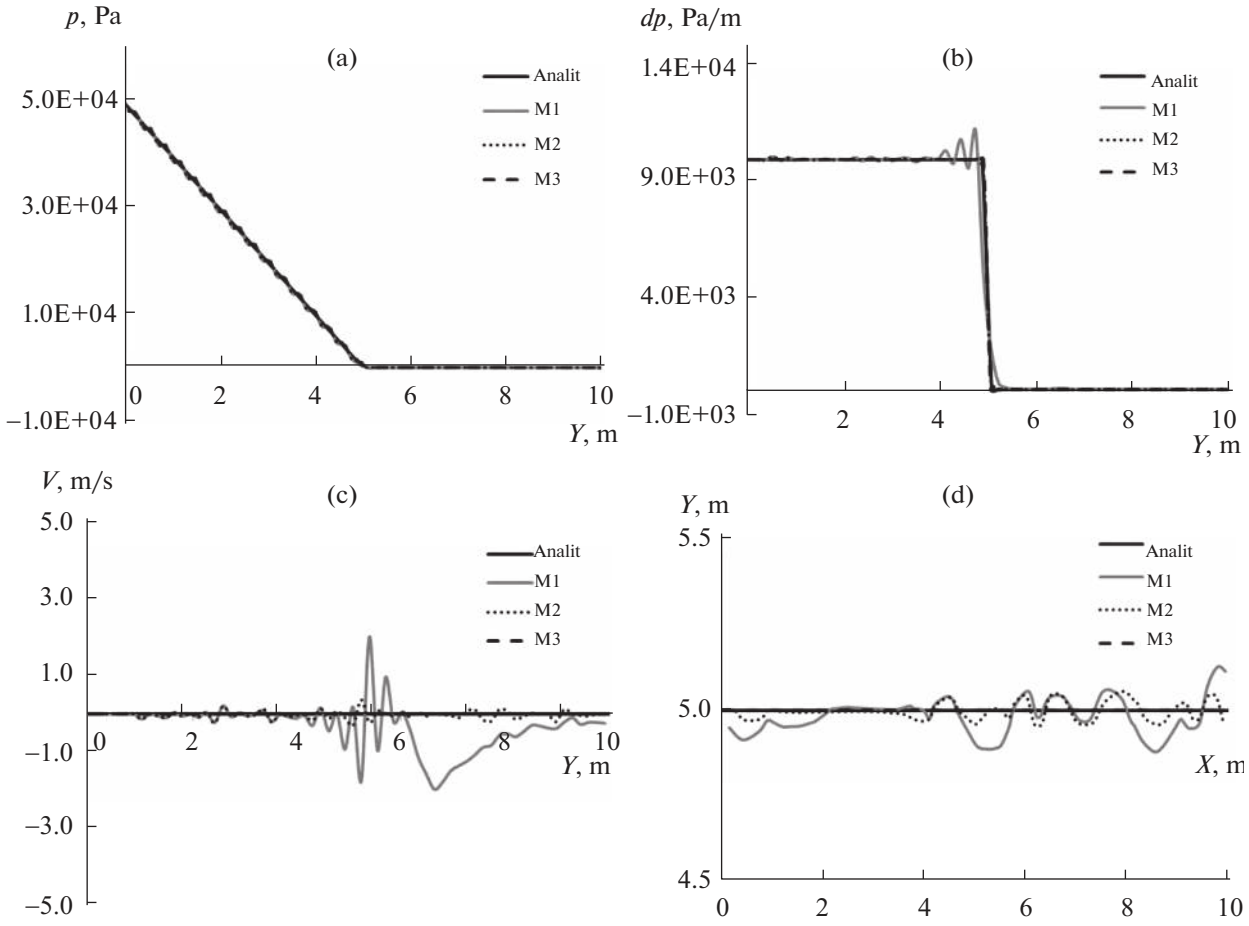

Fig. 5. Plots of (a) pressure, (b) pressure gradient, (c) vertical velocity, and (d) free surface.

for deriving the pressure equation. Using linear interpolation with weight λ_k to compute the face values, we obtain

$$\int_{V_P} \frac{\partial p^*}{\partial x_i} dV \approx \sum_k [\lambda_k [p - \rho g_i (r_i - r_{P,i})]_P + (1 - \lambda_k)[p - \rho g_i (r_i - r_{P,i})]_N] n_{k,i} S_k$$
$$\sum_k [\lambda_k p_P + (1 - \lambda_k)(p - d_{i,Nk} g_i \rho_N - d_{i,kP} g_i \rho_P)_N] n_{k,i} S_k. \quad (2.7)$$

Expression (2.7) has the following physical interpretation. Due to the gravity force ρg_i, the pressure gradient is reduced by the same value that was introduced by ρg_i in deriving pressure equation (1.11). As a result, the pressure gradient is always balanced by the gravity force in the case of a medium at rest.

Below, we present numerical results demonstrating the efficiency of the numerical algorithms proposed for computing the pressure and its gradient in free-surface problems.

3. NUMERICAL EXPERIMENTS

The numerical experiments described below were performed using the software package LOGOS, which is intended for solving three-dimensional coupled problems in convective heat and mass transfer, aerodynamics, and fluid dynamics on parallel computers (see [20–22]). LOGOS has been successfully tested and produced fairly good results on a series of various hydrodynamic problems, including the computation of turbulent and unsteady flows [23–26] and industrial problems [27, 28]. The acceleration of

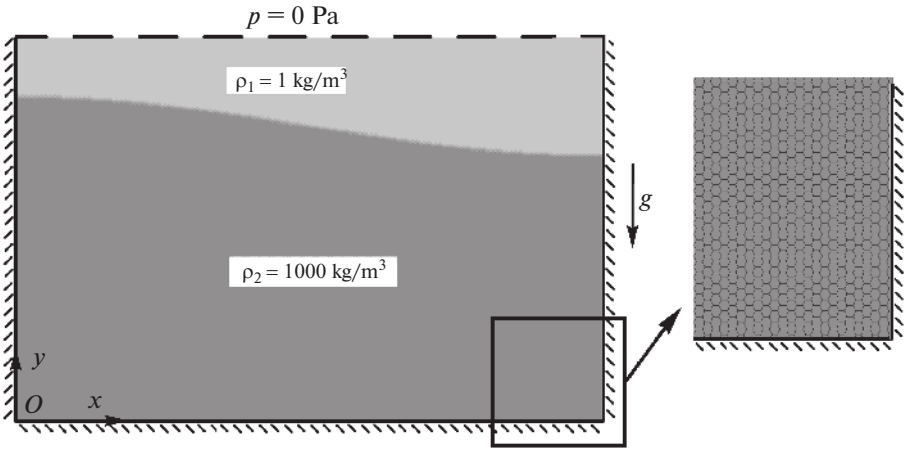

Fig. 6. Conditions of the problem, geometry, and grid.

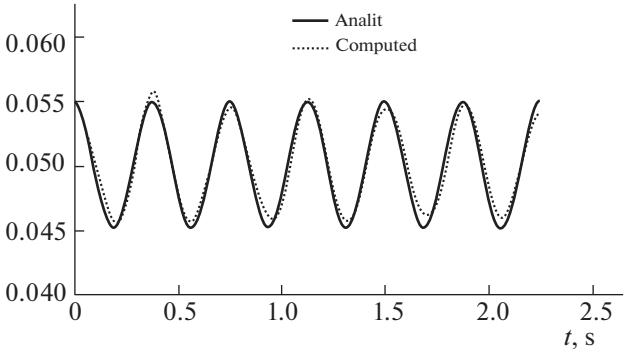

Fig. 7. Free surface position near the left edge of the tank.

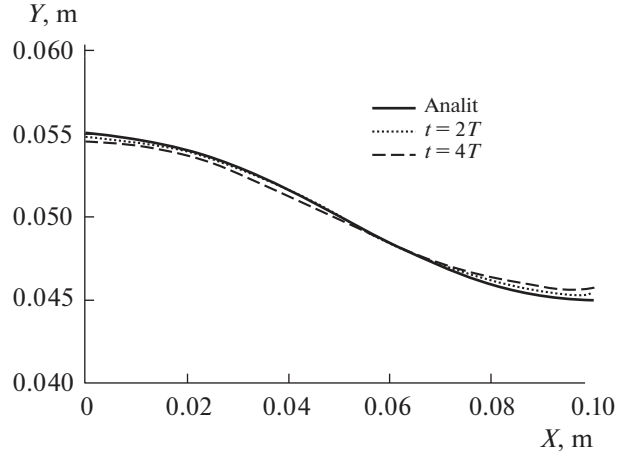

Fig. 8. Free surface shape at various times.

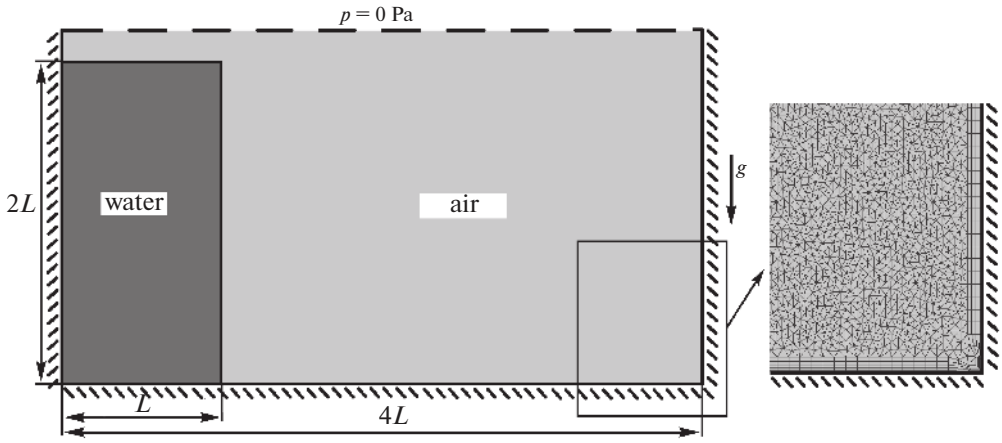

Fig. 9. Initial conditions of the problem, geometry, and grid.

computations with the help of highly parallel computer systems is based on multigrid techniques, a detailed description of which can be found in [29, 30].

3.1. Equilibrium of a Two-Phase Medium under Gravity

Equilibrium of a two-phase medium under gravity is the simplest hydrostatic problem having an analytical solution (see [8]). However, its simulation by applying the VOF method on an unstructured mesh can lead to difficulties caused the discontinuity of the density on the free surface. The problem was considered in a square domain of side length $L = 10$ m. A half of the domain was filled with water at rest. The rest of the tank was occupied by air. Both phases were assumed to be incompressible.

A triangular grid was used to simulate the problem (Fig. 3).

The problem was simulated in two stages. At the first, we tested the efficiency of the numerical schemes for computing pressure, while the efficiency of the numerical schemes for computing the pressure gradient was tested at the second stage.

At the first stage, the velocities were set to zero and the pressure equation was solved using scheme (1.11) (denoted by P1) and the usual scheme (1.4) (denoted by P2). In the scheme P2 on the considered grid under the considered conditions of the problem, the various methods for computing λ_k were reduced to a single one, which was used in the computations:

$$\lambda_k = \frac{d_{Nk}}{d_{Nk} + d_{Pk}} = \frac{a_{NN}}{a_{PP} + a_{NN}} = 0.5.$$

The equations P1 and P2 were solved using an iterative SLAE solver with the relative accuracy $\delta = 10^{-6}$. Figure 4 shows the computed pressure along the central vertical line as compared with the analytical solution.

The method P1 yields good results: the pressure field coincides with the analytical solution. The pressure plot produced by the method P2 has the correct slope in the area of strong pressure variations (the first part of the plot), but the absolute value of pressure has a deviation of about 2 kPa. This discrepancy appears at $Y = 5$ m coinciding with the free surface position and is associated with the incorrect contribution of the gravity force to the pressure equation in the case of a discontinuous medium density.

In what follows, only the method P1 was used at the second stage. Let us discuss the efficiency of the methods for pressure gradient computation. The method based on the Gauss formula (2.1) with linear interpolation of the pressure to a face is denoted by M1, the method (2.2) with modified interpolation of pressure to a face is denoted by M2, and the method of modified pressure gradient (2.7), by M3. The problem was computed over the model time $t = 1$ s with the time step $\Delta t = 0.01$ s. The computed distributions of pressure, pressure gradient, and vertical velocity along the central vertical line are compared with the analytical solution (Fig. 5).

As in the case of the scheme P2, the pressure distribution for each of the methods overall agrees with the analytical solution. However, some discrepancies are observed for M1 and M2, which are associated

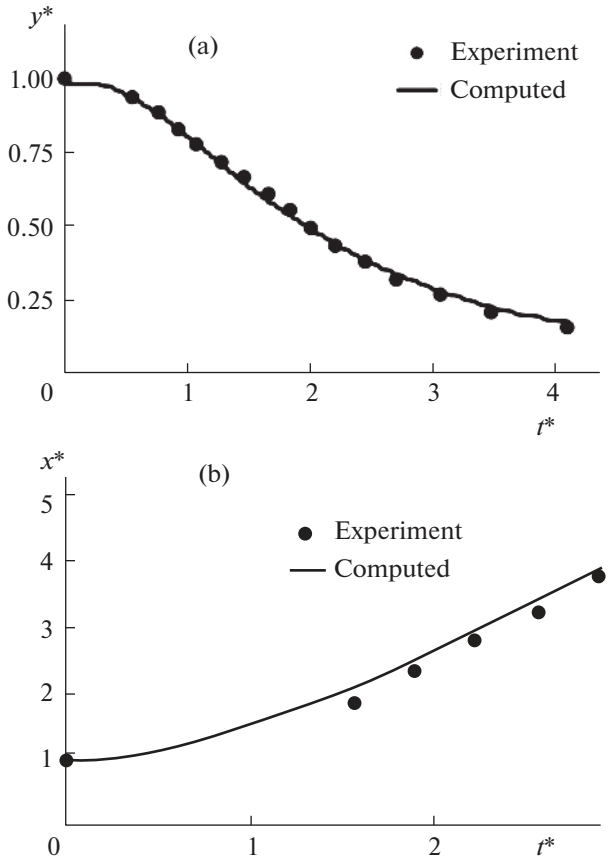

Fig. 10. (a) Water column height and (b) liquid-covered bottom length.

with nonzero vertical velocities arising due to the unbalanced pressure-gradient and gravity forces. These discrepancies are more pronounced in the plot of the pressure gradient. The pressure gradient produced by M1 exhibits oscillations, which are caused by the unbalanced pressure-gradient and gravity forces. The method M2 also leads to some discrepancies in the pressure gradient near the free surface, which are revealed as nonzero vertical velocities (Fig. 5). Due to the modified pressure gradient procedure, the method M3 yields a solution coinciding with the analytical one up to the accuracy of the SLAE solution for pressure.

The plot of the vertical velocity reveals the formation of perturbations for M1 and M2. Eventually, these perturbations lead to a perturbed free surface shape and the generation of spurious waves on it (Fig. 5d). The perturbation amplitudes of the velocity and the free surface shape for M2 are smaller than those for M1. The method M3 yields a maximum vertical velocity on the order of 10^{-7} m/s, which is negligibly low and is explained by the finite accuracy of the SLAE solution for pressure. No distortions of the free surface shape are observed for such vertical velocities.

Thus, in the case of a hydrostatic equilibrium, the pressure and velocity fields produced by M3 on an unstructured grid are free from numerical oscillations near the free surface due to the modified pressure gradient procedure (2.2). The methods M1 and M2 yield oscillations in the vertical velocity field. Over time, they lead to a distorted shape of the free surface and the generation of spurious waves on it. This effect is most pronounced in problems with not very large variations in the free surface shape (wave propagation in stagnant water, etc.).

Below, the accuracy of the free surface shape produced by M3, together with the algorithm P1 taking into account the gravity force in the pressure equation, is estimated as applied to the problem of fluid oscillation under gravity and the breaking liquid column problem.

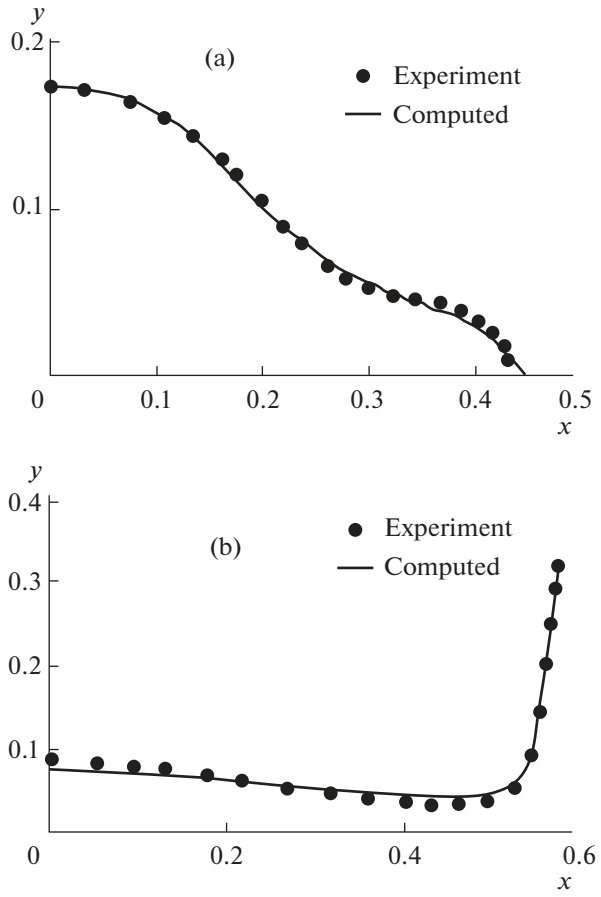

Fig. 11. Free surface shape at (a) $t = 0.2$ s and (b) $t = 0.4$ s.

3.2. Fluid Oscillation under Gravity

Consider the oscillation of an initially perturbed free surface of an inviscid fluid under gravity. The initial perturbation is specified as a half-period of a sinusoidal wave

$$y(x) - 0.05 + 0.005\sin(x\pi/L + \pi/2)\ [\text{m}], \tag{3.1}$$

where $L = 0.1$ m is the length of the tank. This problem has an analytical solution for the oscillation period (see [31]):

$$T = 2\pi\sqrt{gk\tanh(kh)}, \quad k = 2\pi/L.$$

For this configuration, the period is $T = 0.374$ s. At times multiple of T, the free surface shape has to repeat initial perturbation (3.1). The problem was simulated by applying the scheme P1 with the pressure gradient produced by M3. The grid was unstructured and polyhedral with the total number of cells equal to 30000 (Fig. 6).

The computations were performed over the time $t = 10T$ s with $\Delta t = 0.001$ s. The free surface position near the left edge of the tank (Fig. 7) and the free surface shape at various times (Fig. 8) were compared with the analytical solution.

The plot of the free surface position near the left edge of the tank is in good agreement with the analytical solution. However, alternating maximum values are observed, which are associated with a harmonic of period $2T$ present in the oscillation. The same result was observed on a structured grid in [7]. The most probable cause is that the transport equation for the volume fraction of system (1.1) is solved using the numerical scheme M-CICSAM [7], which contracts the phase boundary, thus introducing additional harmonics into the free surface shape.

The free surface shapes at various times agree well with the analytical solution. The maximum relative deviation in the amplitude is 3% at $t = 2T$ and 5% at $t = 4T$, which is comparable in accuracy with the results obtained on structured grids in [7, 17].

3.3. Liquid Column Breaking

Consider the breaking of a liquid column that is initially at rest in a rectangular tank. For this problem, there are experimental data, namely, the free surface shape, the liquid column height near the left edge of the tank, and the liquid-covered bottom length at various times (see [7]). The geometry of the problem and the initial position of the liquid are shown in Fig. 9. The width of the liquid column corresponds to the experiment: $L = 0.146$ m.

The problem was computed on a triangular grid with prismatic boundary layers near the solid surface. The number of grid elements was 37 000 (Fig. 9). The computations were performed over the model time $t = 1$ s with the time step $\Delta t = 0.001$ s. The algorithm P1 (for taking into account the force of gravity in the pressure equation) was used together with M3 (for pressure gradient computation). In Fig. 10, the liquid column height and the liquid-covered bottom length computed in dimensionless parameters are compared with the experimental data.

Here, $y^* = y/2L$, $x^* = x/L$, and $t^* = t(2g/L)^{1/2}$, where y is the height of the liquid column and x is the liquid-covered bottom length. The liquid column height computed with the use of the developed algorithms agrees well with the experimental data. However, the computed velocity of propagation of the liquid over the bottom of the tank (Fig. 10b) is somewhat higher than the experimental values. Figure 11 shows the free surface shape at two times as compared with the experimental free surface recovered from the pictures taken in [7].

The computed free surface shape agrees well with the experimental data. At $t = 0.2$ s, the liquid front near the bottom propagates faster (the same as in the plot of liquid propagation over the bottom). As a result, the liquid level near the left edge of the tank at $t = 0.4$ s becomes understated. Most likely, this effect is associated with the diffusion of the liquid volume fraction near its front at the bottom. The same effect is observed in computations on structured grids [17], so it is not related to the proposed algorithms. Overall, the maximum deviation of the free surface shape from the experiment is at most 6%, while the average deviation is about 3%.

Thus, the above analysis of the problems suggests that the proposed algorithms allow one to correctly describe the evolution of a free surface shape under gravity.

CONCLUSIONS

A numerical algorithm was constructed that correctly takes into account the gravity force and produces pressure gradients in the case of a discontinuous medium density, which always occurs in free-surface problems. A correct hydrostatic pressure field was obtained using an algorithm in which the gravity force contribution is extracted in deriving a pressure equation and is computed by solving the problem of gravitational equilibrium of a two-phase medium. To correctly compute the pressure gradient in the case of a discontinuous gravity field, an algorithm was proposed that produces good results on grids of any type. The basic idea behind the algorithm is based on the direct calculation of the joint contribution made by the pressure gradient and the gravity force to the equation of motion.

The efficiency of the algorithms was checked by computing the equilibrium of a two-phase medium under gravity. It was shown that the algorithm proposed for constructing a pressure equation gives a correct pressure field, while the algorithm for gradient computation ensures that the vertical velocity field is free of numerical oscillations; therefore, there are no distortions in the free surface shape. The accuracy of the free surface shape produced by the proposed algorithms was demonstrated as applied to the problem of fluid oscillation under gravity and liquid column breaking. It was shown that the algorithms yield the correct free surface shape in its evolution under gravity.

The algorithms proposed are applicable in numerical schemes based on unstructured collocated grids and splitting techniques based on SIMPLE, PISO, and similar methods. These algorithms can easily be extended to any other inhomogeneous body force (instead of gravity).

ACKNOWLEDGMENTS

The results presented were obtained by implementing a state task in scientific research (task no. 5.4568.2017/VU (“implementation of scientific studies”) and task no. 5.5176.2017/BCh). This work was

supported by a grant from the President of the Russian Federation for state support of leading scientific schools of the Russian Federation (project no. NSh-6637.2016.5) and by the Russian Foundation for Basic Research (project nos. 15-45-02061 and 16-01-00267).

REFERENCES

1. T. D. Butler, "LINC method extensions," Lect. Notes Phys. **8**, 435–440 (1971).
2. N. G. Burago, Doctoral Dissertation in Mathematics and Physics (Keldysh Inst. of Applied Mathematics, Russian Academy of Sciences, Moscow, 2003).
3. L. B. Lucy, "A numerical approach to the testing of the fission hypothesis," Astron. J. **82** (12), 1013–1024 (1977).
4. F. H. Harlow and J. E. Welch, "Numerical calculation of time-dependent viscous incompressible flow," Phys. Fluids **8**, 2182–2189 (1965).
5. B. J. Daly, "A technique for including surface tension effects in hydrodynamic calculations," J. Comput. Phys. **4**, 97–117 (1969).
6. C. W. Hirt and B. D. Nichols, "Volume of fluid (VOF) method for the dynamics of free boundaries," J. Comput. Phys. **39**, 201–226 (1981).
7. O. Ubbink, PhD Thesis (Imperial College, University of London, London, 1997).
8. L. D. Landau and E. M. Lifshitz, *Fluid Mechanics* (Butterworth-Heinemann, Oxford, 1987; Nauka, Moscow, 1988).
9. J. H. Ferziger and M. Peric, *Computational Method for Fluid Dynamics* (Springer, New York, 2002).
10. H. Jasak, PhD Thesis (Department of Mechanical Engineering, Imperial College of Science, London, 1996).
11. C. A. J. Fletcher, *Computational Techniques for Fluid Dynamics* (Springer-Verlag, Berlin, 1990; Mir, Moscow, 1991)
12. C. M. Rhie and W. L. Chow, "Numerical study of the turbulent flow past an airfoil with trailing edge separation," AIAA J. **21**, 1525–1532 (1983).
13. C. Y. Gu, C. Taylor, and J. H. Chin, "Computation of flows with large body forces," in *Numerical Methods in Laminar and Turbulent Flow* (Pineridge, Swansea, 1991), pp. 294–305.
14. J. Mencinger, "An alternative finite volume discretization of body force field on collocated grid," *Finite Volume Method: Powerful Means of Engineering Design* (2012), pp. 101–116.
15. A. I. Khrabry, Candidate's Dissertation in Mathematics and Physics (St. Petersburg State Univ., St. Petersburg, 2015).
16. S. Majumdar, "Role of underrelaxation in momentum interpolation for calculation of flow with nonstaggered grids," Numer. Heat Transfer **13**, 125–132 (1988).
17. S. V. Yatsevich, V. V. Kurulin, and D. P. Rubtsova, "The PISO algorithm as applied to problems in the dynamics of molecularly immiscible liquids," Vopr. At. Nauki Tekh., Ser. Mat. Model. Fiz. Protsessov, No. **1**, 16–29 (2015).
18. A. I. Khrabry, E. M. Smirnov, and D. K. Zaytsev, "Solving the convective transport equation with several high-resolution finite volume schemes: Test computations," *Computational Fluid Dynamics 2010* (Springer, Berlin, 2011), pp. 535–540.
19. A. A. Kurkin, A. S. Kozelkov, and D. P. Meleshkina, "Fully implicit Navier–Stokes solver for free-surface multiphase flow computations," *Proceedings of the 11th All-Russia Conference on Fundamental Problems in Theoretical and Applied Mechanics, Kazan, August 20–24, 2015* (Kazan, 2015), pp. 1851–1852.
20. A. S. Kozelkov, A. A. Kurkin, and E. N. Pelinovskii, "Modeling of a body falling into water under various conditions by applying a fully implicit Navier–Stokes solver," Tr. Nizhegorod. Gos. Tekh. Univ. im. R.E. Alekseeva, No. **3**, 51–69 (2015).
21. A. S. Kozelkov, A. A. Kurkin, E. N. Pelinovskii, and V. V. Kurulin, "Modeling the cosmogenic tsunami within the framework of the Navier–Stokes equations with sources of different types," Fluid Dyn. **50** (2), 306–313 (2015).
22. A. S. Kozelkov, A. A. Kurkin, and E. N. Pelinovskii, "Effect of the angle of water entry of a body on the generated wave heights," Fluid Dyn. **51** (2), 288–298 (2016).
23. A. S. Kozelkov, A. A. Kurkin, V. V. Kurulin, M. A. Legchanov, E. S. Tyatyushkina, and Yu. A. Tsibereva, "Investigation of the application of RANS turbulence models to the calculation of nonisothermal low-Prandtl-number flows," Fluid Dyn. **50** (4), 501–513 (2015).
24. A. Kozelkov, V. Kuralin, V. Emelyanov, E. Tyatyushkina, and K. Volkov, "Comparison of convective flux discretization schemes in detached-eddy simulation of turbulent flows on unstructured meshes," J. Sci. Comput. **89**, 1–16 (2015).
25. A. S. Kozelkov and V. V. Kurulin, "Eddy-resolving numerical scheme for simulation of turbulent incompressible flows," Comput. Math. Math. Phys. **55** (7), 1232–1241 (2015).

26. A. S. Kozelkov, A. A. Kurkin, O. L. Krutyakova, V. V. Kurulin, and E. S. Tyatyushkina, "Zonal RANS–LES approach based on an algebraic Reynolds stress model," Fluid Dyn. **50** (5), 621–628 (2015).
27. M. A. Pogosyan, E. P. Savel'evskikh, P. M. Shagaliev, D. Yu. Strelets, A. A. Ryabov, A. V. Kornev, Yu. N. Deryugin, V. F. Spiridonov, and K. V. Tsiberev, "Domestic supercomputer technologies as applied to the design of prospective aircrafts," Vopr. At. Nauki Tekh., Ser. Mat. Model. Fiz. Protsessov, No. **2**, 3–17 (2013).
28. M. A. Pogosyan, E. P. Savel'skikh, D. Yu. Strelets, and A. V. Kornev, "Domestic supercomputer technologies in the aviation industry," Nauka Tekhnol. Promyshl., No. 2, 26–35 (2012).
29. A. S. Kozelkov, Yu. N. Deryugin, S. V. Lashkin, D. P. Silaev, and P. G. Simonov, "Implementation of a multigrid method based on the SIMPLE algorithm in the application package LOGOS for viscous incompressible flow computations," Vopr. At. Nauki Tekh., Ser. Mat. Model. Fiz. Protsessov, No. **4**, 44–56 (2013).
30. K. N. Volkov, Yu. N. Deryugin, V. N. Emel'yanov, A. G. Karpenko, A. S. Kozelkov, and I. V. Teterina, *Methods for Acceleration of Gasdynamic Computations on Unstructured Meshes* (Fizmatlit, Moscow, 2013) [in Russian].
31. P. E. Raad, S. Chen, and D. B. Johnson, "The introduction of micro cells to treat pressure in free surface fluid flow problems," J. Fluids Eng. **117**, 683–690 (1995).

Translated by I. Ruzanova

SPELL: OK